Arab J Sci Eng (2014) 39:7957–7965
DOI 10.1007/s13369-014-1324-z

RESEARCH ARTICLE - ELECTRICAL ENGINEERING

A Swarm-Based Adaptive Neural Network SMES Control for a Permanent Magnet Wind Generator

A. H. M. A. Rahim · M. H. Khan

Received: 16 December 2013 / Accepted: 30 April 2014 / Published online: 29 August 2014

Abstract Permanent magnet synchronous generators are becoming increasingly popular as utility-scale wind generators. While their performances are satisfactorily under normal conditions, they may be degraded under wind gusts as well as in extremely low grid voltage conditions. An adaptive control of superconducting magnetic energy storage (SMES) system for efficient wind energy transfer as well as dynamic performance improvement is proposed in this article. A radial basis function neural network has been employed to determine the controller parameter values. The nominal weights of the neural network are obtained from training of a large input-output data set generated through an improved swarm optimization procedure. These weights are then updated through a novel method of tracking of system outputs in time domain. Tests carried out with the adaptive controller show that the improved particle swarm-based radial basis network SMES controller delivers wind energy to grid efficiently and at the same time exhibit very good damping profile.

Keywords Adaptive neural network · Radial basis function · Particle search optimization · PMSG · SMES · Wind generator

A. H. M. A. Rahim (✉)
Department of Electrical Engineering, King Fahd University of Petroleum and Minerals, Dhahran, Saudi Arabia
e-mail: Ahrahim@kfupm.edu.sa; ahrahim@hotmail.com

M. H. Khan
Department of Strategic and Planning, Saudi Electricity Company, Dammam, Saudi Arabia
e-mail: muhammadharisk@gmail.com

الخلاصة

تُعدّ المولدات ذات المغناطيس الدائم في ازدياد مولداتٍ هوائية واسعة الانتشار. لقد وجد أن أداء هذه المولدات مقبول تحت الظروف العادية، ولكنه يقل مع الرياح المحملة بالرمال، وعند خفض جهد الشبكة. يقترح هذا البحث حلاً لهذه المشكلة باستخدام منظم تحكم يعتمد على موصل مثالي يخزن الطاقة المغناطيسية. وقد استخدم دالة دائرية في الشبكة العصبية لإيجاد البارامترات اللازمة لتصميم منظم التحكم المقترح. وحتى نحصل على أفضل قيم لشبكه العصبية تم تدريب الشبكة باستخدام كمية كبيرة من البيانات من خلال طريقة المثالي التي تعتمد على الأسراب. وتم كذلك ابتكار طريقة جديدة لتحديث القيم المستخدمة في الشبكة العصبية من خلال ملاحظة مخرجات النظام في النطاق الزمنى. وتمت أيضاً تجربة منظم التحكم لبيان التحسن عند استخدام داله دائرية في الشبكة العصبية لتغزية طاقة الرياح وتأثيرها في أداء الشبكة. وقد لوحظ في الوقت نفسه أن منحنى الاضمحلال أصبح جيد جدا.

1 Introduction

Permanent magnet synchronous generator wind turbines are being widely used in industry because of their simplicity in structure, efficiency of energy production, high torque-weight ratio, brushless excitation, etc [1,2]. In the PMSG configuration, the generated variable frequency voltage is converted to the grid frequency through two full-scale converters connected back-to-back with a DC capacitor in between. This also provides isolation between the two synchronous systems [3]. However, under random wind speed variations, the fluctuation in power may get past the converters and cause problems in grid frequency, especially in a weak grid [1,4].

Various methods of frequency and voltage stabilization of PMSG generators under varying wind speed conditions have been reported in the literature. Control of the converter on the generator side was used in [5] to reduce voltage sag, while [6] employed control of grid side converter for maximizing transfer of wind power. Reference [7] used control

of both the converters, the generator side one for improving the power transfer and the grid side converter for reactive control. Energy storage devices interfaced through electronic flexible ac transmission system (FACTS) are known to improve the system performance by compensating the reactive power need of the system. Use of STATCOM with PID control was observed to improve the damping properties of a PMSG [8], while STATCOM and battery energy storage was used by Sharma for voltage and frequency control [9]. Battery energy storage along with fuel cell and dump resistor was used for reducing torque pulsation in a grid connected PMSG system [10]. SMES can supply both reactive and real power and hence can affect both voltage and frequency profiles [11,12]. Most of the control designs are carried out in the linear domain employing PI or PID controllers. Linear designs, while can give very good results in the vicinity of the operating points, are generally not satisfactory for wind generators which experience random wind speed changes. For satisfactory performance, the controller parameters should also be adaptively tuned in time domain so as to respond to random and arbitrary changes. Considering the erratic nature of wind, use of intelligent control strategies has been recommended in the literature [13]. Betzel [14] used neural network control for rotor angle estimation in PMSG systems. A combination of sliding mode and radial basis function networks was employed for pitch control in [15]. The control designs are generally carried out from a fixed weighting function obtained from data training. However, adaptive controller design of SMES for wind generator performance improvement has not been addressed in the literature.

This article presents an adaptive neural network SMES controller design for a PMSG wind generator. The adaptive technique updates the neural network weights in time domain. The radial basis network function network employed has better capability of approximation and faster learning speed [16]. A modified particle swarm method generates the optimized nominal weights of the neural network. Section 2 of the article gives the wind system model including SMES controller, and Sect. 3 presents the adaptive RBFNN SMES controller design. Section 4 presents the test results, and concluding remarks are given in Sect. 5.

2 Dynamic Model

The permanent magnet wind generator system considered in this article is shown in Fig. 1. The variable frequency voltage generated by the PMSG is rectified and inverted to grid frequency through fully controlled converters. The voltage is stepped up before being fed to the grid over the transmission line. The local load and the proposed SMES system are connected at the inverter terminal. Models of the PMSG, the drive train, the converters, and the SMES system are summarized below.

2.1 PMSG and the Converters

The dynamic relationships of the PMSG stator circuit voltage, current, and flux along the direct and quadrature (d–q) axes are expressed through,

$$\begin{aligned} -R_{\mathrm{a}} i_{\mathrm{gd}} - \omega_{\mathrm{g}} \psi_{\mathrm{q}} + \frac{1}{\omega_{\mathrm{o}}} p\left(\psi_{\mathrm{d}}\right) &= V_{\mathrm{gd}} \\ -R_{\mathrm{a}} i_{\mathrm{gq}} + \omega_{\mathrm{g}} \psi_{\mathrm{d}} + \frac{1}{\omega_{\mathrm{o}}} p\left(\psi_{\mathrm{q}}\right) &= V_{\mathrm{gq}} \end{aligned} \tag{1}$$

$$\begin{aligned} \psi_{\mathrm{d}} &= -x_d i_{\mathrm{gd}} + \psi_{\mathrm{o}} \\ \psi_{\mathrm{q}} &= -x_q i_{\mathrm{gq}} \end{aligned} \tag{2}$$

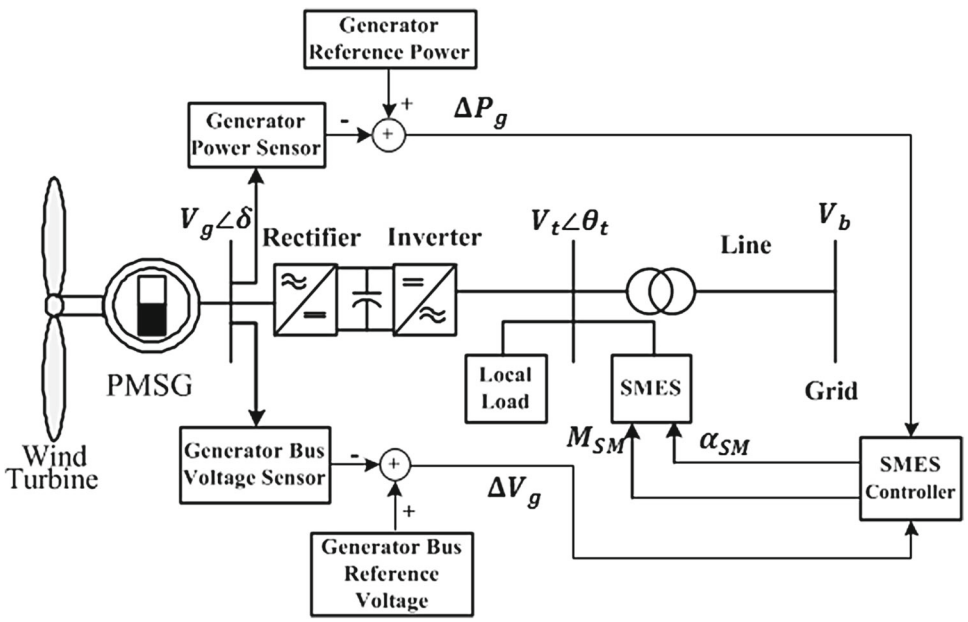

Fig. 1 Schematic of PMSG system connected to the grid

In the above equations, V_{gd} and V_{gq} are the components of generator terminal voltage V_g; R_a, x_d, x_q are the stator resistance, synchronous reactances, respectively, and ψ_o is the residual flux from the permanent magnets. The dynamic equations of the turbine-generator rotor mass drive train model are expressed as [17],

$$\begin{aligned}\dot{\omega_t} &= \frac{1}{2H_t}[P_m - K_s\theta_s - D_t(\omega_t - 1)]\\ \dot{\omega_g} &= \frac{1}{2H_g}[K_s\theta_s - P_e - D_g(\omega_g - 1)]\\ \dot{\theta_s} &= K_s(\omega_t - \omega_g)\end{aligned} \tag{3}$$

The power input to the generator, which is the turbine output, relates to wind velocity (V_w) and power coefficient (C_p) through,

$$P_m = K_p V_w^3 C_p \tag{4}$$

Constant K_p depends on area covered by the blade and density of air. C_p is expressed in terms of tip speed t_s and pitch angle α_p through the nonlinear relation,

$$\begin{aligned}C_p(t_s, \alpha_p) &= 0.5176\left(\frac{116}{\psi} - 0.4\alpha_p - 5\right)e^{\frac{-21}{\psi}} + 0.0068t_s\\ \frac{1}{\psi} &= \frac{1}{t_s + 0.08\alpha_p} - \frac{0.035}{t_s^3 + 1}\end{aligned} \tag{5}$$

If the converters are considered to be lossless, the voltage equation for the DC link capacitor (V_c) can be derived in terms of capacitance and the input and output power of the capacitor as,

$$C\dot{V_c} = \frac{(P_{ic} - P_{oc})}{V_c} \tag{6}$$

The differential equations relating the d–q components of inverter current are written as,

$$\begin{aligned}\dot{i}_{id} &= \frac{\omega_O}{x_i}(V_{id} - V_{td} - R_i i_{id} + \omega x_i i_{iq})\\ \dot{i}_{iq} &= \frac{\omega_O}{x_i}(V_{iq} - V_{tq} - \omega x_i i_{id} - R_i i_{iq})\end{aligned} \tag{7}$$

V_i and V_t are the internal and terminal voltages of the inverter, respectively.

2.2 Superconducting Magnetic Energy Storage (SMES) System

The SMES system comprises of a superconducting coil (SC), a buck-boost converter, a VSC, and their control circuitry. The buck-boost converter can make the SC supply or absorb power by control of the IGBT switching. The duty ratio of the converter also affects the reactive power supply. The circuit arrangement of the SMES system is shown in Fig. 2.

The change in the SMES current is expressed in terms of the terminal ac voltage and delay angle is [11],

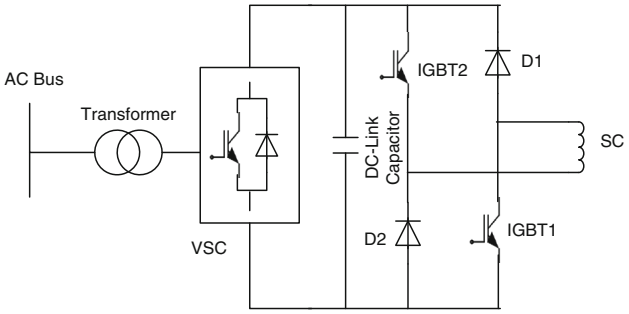

Fig. 2 The superconducting energy storage system

$$L_{sc}\Delta\dot{I}_{sm} = -\Delta I_{sm}R_{sc} + V_t\cos\alpha_{sm} - (\pi/12)\Delta I_{sm}X_{cm} \tag{8}$$

L_{sc}, R_{sc}, and X_{cm} are the inductance and resistance of the SC, and commutation reactance, respectively. Denoting the VSC voltage and SMES current as $V_t\angle\theta_t$, $I_{sm}\angle\alpha_{sm}$, the d–q components of SMES current i_{smd}, i_{smq}), the real and reactive power (P_{SM}, Q_{SM}) are,

$$\begin{aligned}i_{smd} &= m_{sm}I_{dc}\cos(\theta_t - \alpha_{sm})\\ i_{smq} &= m_{sm}I_{dc}\sin(\theta_t - \alpha_{sm})\end{aligned} \tag{9}$$

$$\begin{aligned}P_{SM} &= v_{td}i_{smd} + v_{tq}i_{smq}\\ Q_{SM} &= v_{td}i_{smq} - v_{tq}i_{smd}\end{aligned} \tag{10}$$

In Eqs. (9), (10) m_{sm} and α_{sm} are the modulation index and delay angle, which are related to SMES voltage, current and power through,

$$m_{sm} = \frac{\sqrt{P_{SM}^2 + Q_{SM}^2}}{V_t I_{dc}} \qquad \alpha_{SM} = \tan^{-1}\left[\frac{Q_{SM}}{P_{SM}}\right] \tag{11}$$

The SMES controller shown in Fig. 3 is designed on the principle that SMES power will change depending on the change in real power of the wind system, while Q_{SM} change will be affected by the change in system voltage.

Combining Eqs. (1, 3, 6–8) with the controller model in Fig. 3, the system dynamic equations are written as,

$$\begin{aligned}\dot{x} &= f[x, u]\\ y &= g[x, u]\end{aligned} \tag{12}$$

In the above, $x = [i_{gd}, i_{gq,}\omega, \theta_s, \omega_t, V_c, i_{id}, i_{iq}, \Delta I_{sm}, \Delta P_{sm}, \Delta Q_{sm}]$. The parameter vector $[K_{PG}, K_{IG}, K_{PV}, K_{PI}]$ constitute the input vector u which are obtained by the adaptive neural network technique presented in the next section; y is a vector of selected output of the system.

3 Adaptive SMES Control Strategy

For getting satisfactory response for the wind system, the PI gain of the controller in Fig. 3 should be tuned appropriately for randomly varying wind speed conditions and also for

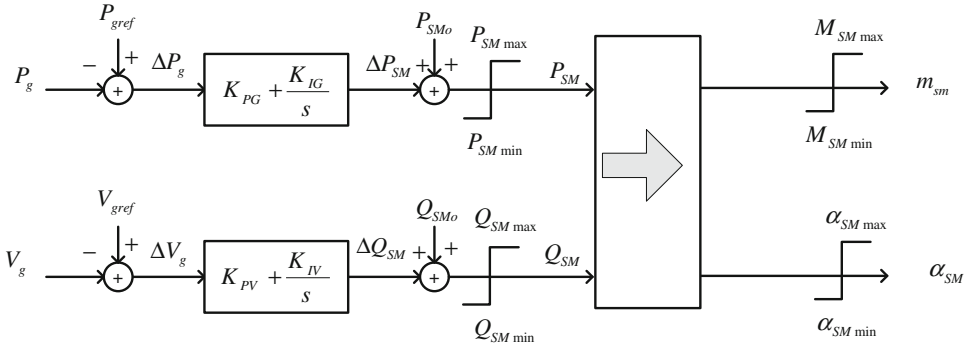

Fig. 3 SMES controller block diagram

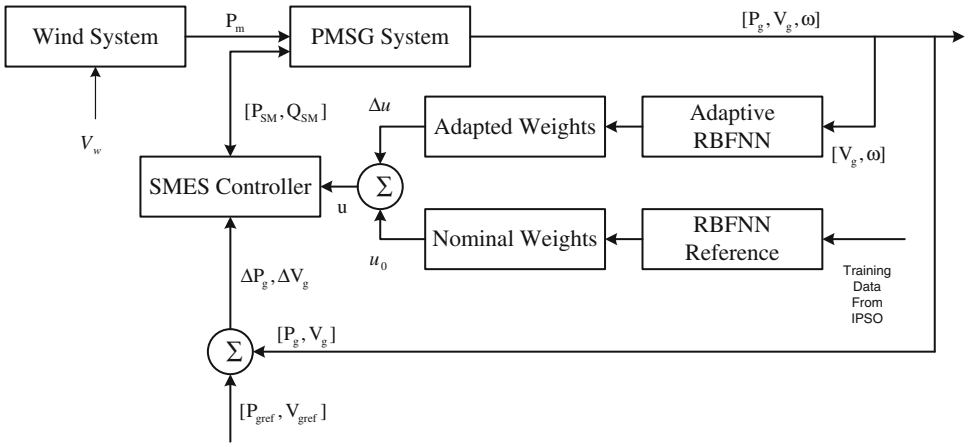

Fig. 4 The adaptive SMES controller structure

other arbitrary disturbances. This article addresses the determination of these gains and their adaptation process through the following procedures:

(a) Determine the controller gains for specific operating conditions using an improved particle swarm optimization (IPSO) evolutionary process.
(b) Determine the nominal weights (w_0) of the radial basis neural network by training the input-output dataset presented by IPSO. The nominal weights are used to produce nominal control u_0, which are the nominal values of parameters [K_{pg}, K_{vg}, T_{pg}, T_{vg}].
(c) Tune the parameters of the controller adaptively in time domain through changes in neural network weights Δw, which produces the changes Δu. The updated control parameters are then obtained as,

$$u(t) = u_o + \Delta u \tag{13}$$

The structure of the adaptive process showing the wind system, PMSG, SMES, and the RBFNN controllers is given in Fig. 4. As can be seen, the control u is generated through two channels. The lower channel generates the nominal control from the nominal weights of the RBFNN network using routine data training. These nominal values stabilize an otherwise unstable system, or systems which are vulnerable to large and unpredictable changes [18]. The inputs to the neural network in the upper track are the PMSG outputs *viz.* terminal voltage and speed. The adaptive neural network is trained to respond to variations in these signals and generate an appropriate weight Δw, which is added to the nominal values to produce the updated controller parameters [K_{pg}, K_{vg}, T_{pg}, T_{vg}]. The process of adaptive update is presented in Sect. 3.1. The SMES control circuit, shown in Fig. 3, uses the PMSG system power (Pg), voltage (Vg), and the updated controller parameters to yield the m_{sm} and α_{sm} signals. The parameter tuning process and hence variations in SMES real and reactive power (P_{SM}, Q_{SM}) is continued until the selected PMSG output variables are returned to their desired steady state values.

The proposed adaptive RBFNN control design procedure and also IPSO technique used in this article are presented below.

3.1 Adaptive Radial Basis Function Network

The adaptive control design using neural network is carried out in two phases. In phase one, a reference RBFNN network, as shown in the lower RBFNN block in Fig. 5, is trained to generate a nominal weighting matrix. The training is con-

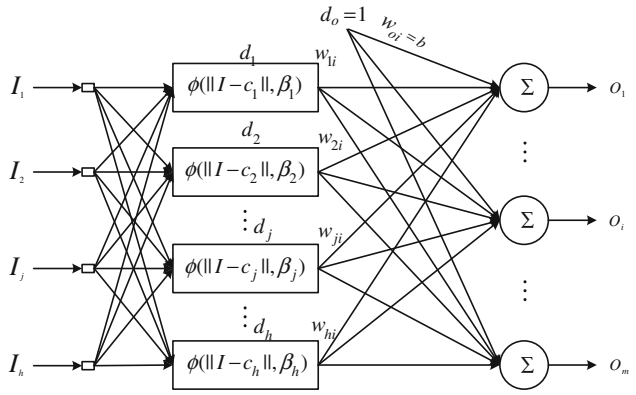

Fig. 5 RBFNN structure

ducted with a large set of input-output data, the input being states at different operating conditions and the output of the network are the controller parameters.

The structure of the RBFNN network is shown in Fig. 5. The output of the network relate to input through,

$$O_i = \sum_{j=1}^{h} w_{ji}\varphi(||I_j - c_j||, \beta_j) + w_{0i} \tag{14}$$

The nonlinear radial basis function $\varphi(.)$ is normally assumed to be a Gaussian. The constant β is the spread of the basis function and c_j is the center of the jth node. Weight w_{ji} at the $(k+1)$th iteration is computed through the recursive formula derived through the well-established least-mean-squares (LMS) algorithm as [19],

$$w_{ji}(k+1) = w_{ji}(k) - \eta \frac{\partial E(k)}{\partial w_{ji}(k)} \tag{15}$$

Here, η is the learning rate parameter. For target output d, the mean squared error at any iteration k, and the gradient are,

$$\begin{aligned} E &= \frac{1}{2}\sum_{j=1}^{N} e_j^2; \quad e_j = d_j - O_j \\ \frac{\partial E(k)}{\partial w(k)} &= -\sum_{j=1}^{N} e_j(k)\varphi\left(\left\|I_j - c_j\right\|, \beta_j\right) \end{aligned} \tag{16}$$

The RBF network was presented with 800 input-output data sets which were created by the IPSO optimization algorithm. The algorithm converged to an error of about 0.01 in about 1,625 epochs.

The adaptive procedure proposed in this work updates the nominal weights in time domain through,

$$w(t_k) = w_{\text{nom}} + \Delta w(t_k) \tag{17}$$

The variation $\Delta w(t_k)$ is obtained by gradient descent method,

$$\begin{aligned} \Delta w(t_k) &= -\eta_2 \frac{\partial \xi}{\partial w_j} = -\eta_2 e_c \frac{\partial e_c}{\partial w_j} \\ &= \eta_2 (r - y)\varphi(||I - c_j||, \lambda) \end{aligned} \tag{18}$$

Here, the error function minimized is,

$$E(t) = \frac{1}{2}\sum e_c^2(t); \quad e_c(t) = r(t) - y(t) \tag{19}$$

In the above, the error $e_c(t)$ is the difference between the system reference output $r(t)$ and the actual plant output $y(t)$ can be obtained from (12). At every time step t_k, the updated weights (17) generate the adaptive control through relation (13).

3.2 Modified Swarm Optimization Algorithm

The input–output training data to generate the nominal weights (w_0) are created by a modified particle swarm optimization procedure. In the improved method, each particle in the swarm updates its velocity and position by updating the inertia weight. For the evaluation of each particle, the following eigenvalue-based fitness function is considered,

$$J = \sum_{i=1}^{N} (\zeta(k) - \zeta_o)^2; \quad \zeta = \frac{-\sigma}{\sqrt{\sigma^2 + \beta^2}} \tag{20}$$

Here, ζ_o is a preselected value of damping ratio: σ and γ are components of the dominant eigenvalue of the linearized system of (12), and N is the total number of iterations.

For getting a faster convergence, exploration and exploitation of the swarm algorithm has to be considered. Exploration is the ability of the algorithm to explore the entire search space. Exploitation is the ability that focuses on an optimum area and refines the solution. The particle velocity and position is accelerated through an inertia weight (w_{in}) expressed as [20],

$$w_{\text{in}} = w_{\max} - \left(\frac{w_{\max} - w_{\min}}{i_{\text{tmax}}}\right) i_{\text{t}} \tag{21}$$

In the above, i_{t} is the current count, and $w_{\max}$, $w_{\min}$, i_{tmax} represent the maximum and minimum values of the weight and maximum iterations, respectively. The expressions for velocity (v) and position (θ) for each particle with improved inertia weight are written as,

$$\begin{aligned} v_{\text{i}}(k+1) &= w_{\text{in}} v_{\text{i}}(k) + c_1 \text{rand}_1(p_{\text{i}}(k) - \theta_{\text{i}}(k)) \\ &\quad + c_2 \text{rand}_2(p_g(k) - \theta_i(k)) \\ \theta_{\text{i}}(k+1) &= \theta_{\text{i}}(k) + v_{\text{i}}(k) \end{aligned} \tag{22}$$

Here, k is iteration number, c_1 and c_2 are the acceleration constants; p_{i} and p_{g} are the local best and global best, respectively. The steps involved in the search procedure are as follows: define search area and boundaries, generate array of particles with random position and velocities, find the local best from evaluation of fitness function, compare local best

with global best, update the weighs, and repeat the procedure until convergence or termination criteria are met.

4 Testing the Adaptive Controller

The proposed adaptive SMES controller was tested on the grid connected PMSG system of Fig. 1. The generator is considered to be delivering 0.95 pu power for wind speed of 10 m/s. The parameter values for the wind generator system are provided in the appendix. For testing the performance of the adaptive SMES controller, all other controls of the converters are deactivated. Also, the generator turbine damping was considered to be zero to simulate a worse-case scenario. Only those disturbances which lead to growing oscillations without any control have been reported in this paper. The contingencies considered are as follows:

- Torque pulses of various magnitude and duration
- Low voltage condition on the grid
- Wind gust

Figure 6 shows the speed variations of the synchronous generator when subjected to a 0.2 pu input torque pulse for 0.3 s duration. The torque unbalance in the generator causes the speed to creep up without any control and in the absence of system damping. The SMES controller supports the system with necessary real and reactive power following the disturbance and helps restore stable operation very quickly as can be observed in Fig. 6. Maintenance of the DC capacitor voltage to a constant level is the essential part in satisfactory operation of the wind generation system. Figure 7 shows that while without any control the capacitor voltage is oscillatory, the proposed adaptive SMES control provides smooth voltage profile and steady conditions are reached in less than 4 s.

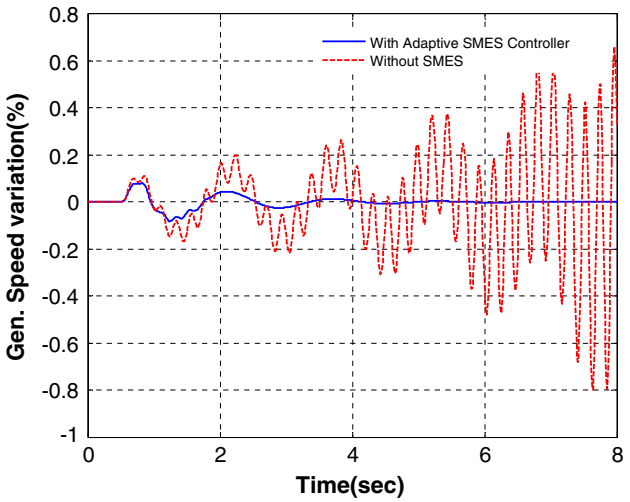

Fig. 6 Variation of generator speed following a 20 % torque pulse for 0.3 s

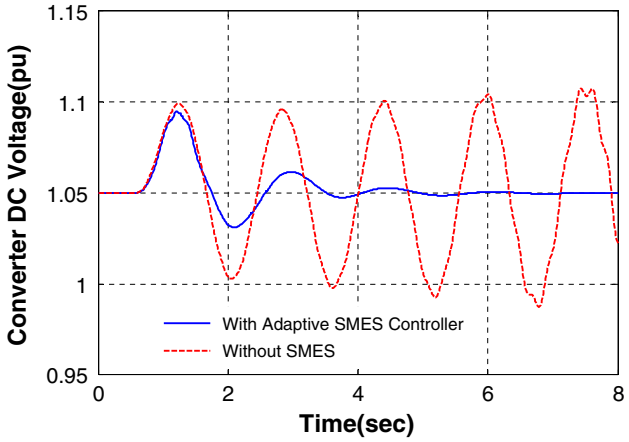

Fig. 7 Variation in voltage of the DC link capacitor for 20 % torque pulse

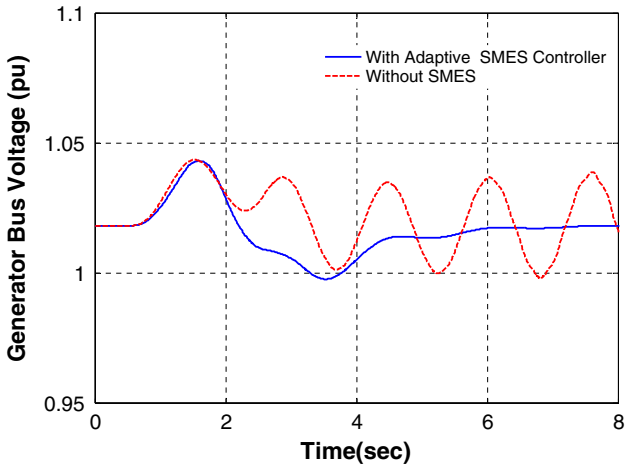

Fig. 8 Permanent magnet synchronous generator terminal voltage variation following a 10 % torque pulse for 2 s, with and without SMES control

For a 10 % torque pulse for 2 s, the generator terminal voltage is depicted in Fig. 8. Without any control, the generator terminal voltage is oscillatory and is slightly growing in the zero damping situation. The proposed adaptive SMES control restores normal terminal voltage fairly quickly for this relatively longer duration disturbance. The variations of SMES reactive and real power output are depicted in Fig. 9. The reactive power of the SMES system helps to stabilize the voltage while real power provides the damping.

Performance of the proposed adaptive SMES controller under grid low voltages was tested by applying a severe 3-ϕ phase fault on the grid bus. Figure 10 shows the variation of the terminal voltage of the synchronous generator for a 300 ms grid fault. The short circuit at the grid depresses the inverter terminal voltage affecting the generator terminal voltage and output power. After the fault is cleared inverter terminal voltage restores quickly but the generator oscilla-

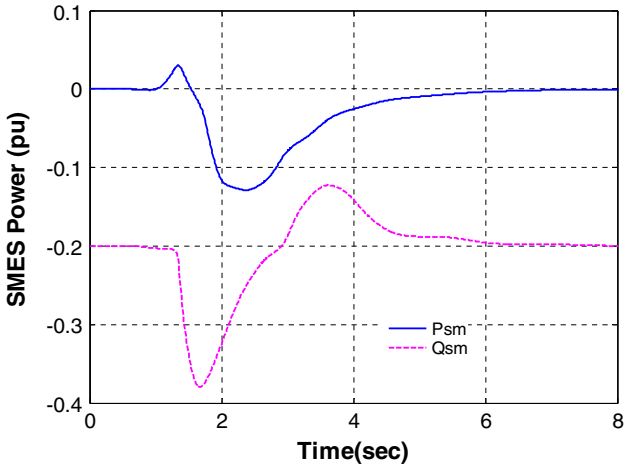

Fig. 9 Change of SMES real and reactive power for the disturbance condition of Fig. 8

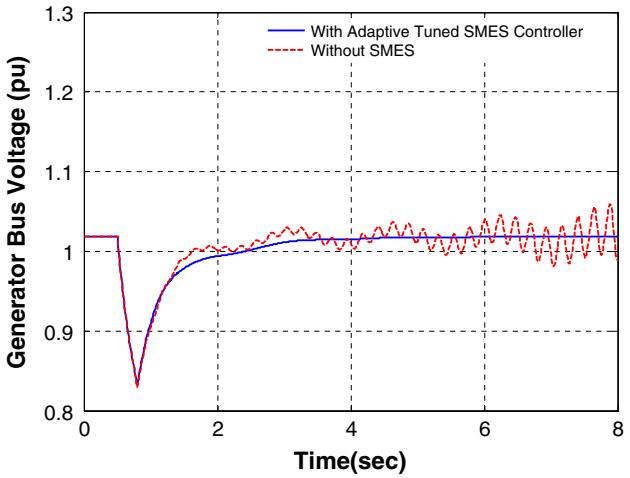

Fig. 10 Synchronous generator bus voltage for a 300 ms grid fault without and with the proposed control

tions continue (Fig. 10). The adaptive controller restores the terminal voltage by the reactive injection of the SMES.

The robustness of the proposed controller was tested with a part of wind data collected from local measurements. The wind speed fluctuations was normalized, scaled, and superimposed on the average value of 10 m/s. Figure 11 shows the generator power with and without the adaptive SMES controller and compares it with the turbine output. Random wind speed variation for 2 s is considered in the simulation and post-disturbance response has been observed. Quick restoration of the DC capacitor voltage (Fig. 12) with the adaptive variation of controller parameters (Fig. 13) provides the excellent power transfer profile shown in Fig. 11.

Examination of Fig. 11 shows that the output of the PMSG follows the input extremely closely in the presence of the proposed SMES control. However, exact evaluation of the efficiency under the transient condition is not easy because

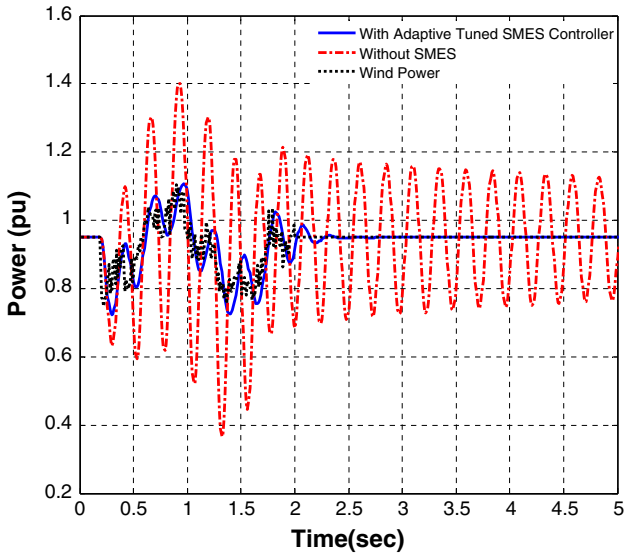

Fig. 11 Wind and generator power output following a 2 s random wind speed variation

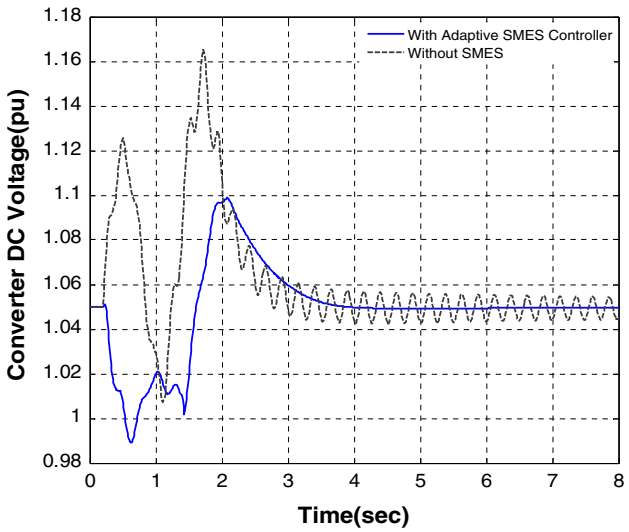

Fig. 12 Converter circuit DC capacitor voltage variation corresponding to a wind speed condition of Fig. 11

of the time lags involved. Also, transiently the output power can be more than the input for short durations. It is more so in the uncontrolled condition when the system falls into sustained oscillation. Since the SMES is lossless, and also since the generator and the converters are considered to be lossless in this study, under steady state the turbine output to converter output efficiency is almost 100 %. The performance of the controller has been evaluated through the computation of the power coefficient C_p (Eq. 4), optimum value of which is known to be slightly less than 0.5. For wind speed variation of between 10 and 11 m/s and then back to 10 m/s, the changes affected in staircase steps, the variation of power coefficient C_p is plotted in Fig. 14. It can be seen that following the

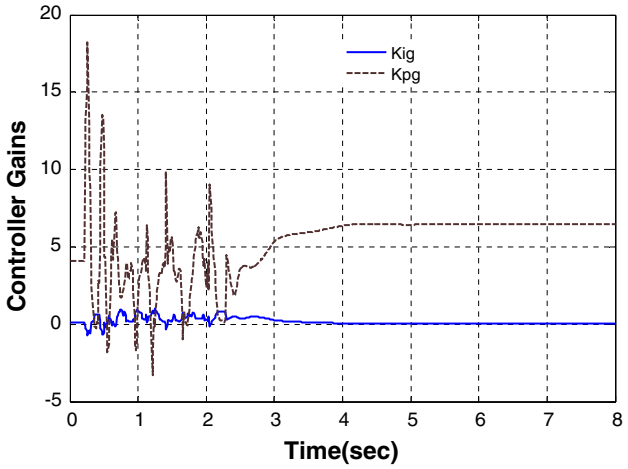

Fig. 13 Variation of the SMES controller parameters

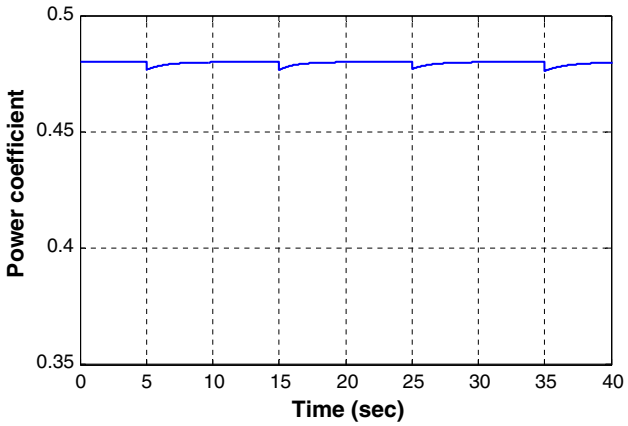

Fig. 14 The variation of power coefficient (C_p) for wind speed variations between 10 and 11 m/s

speed change a ripple appears in C_p, which returns back to optimum value of about 0.48 fairly quickly. This shows that the controller is capable of near optimum transfer of wind power.

5 Conclusions

A novel adaptive SMES controller for a grid connected PMSG is proposed in this study. The controller parameters are tuned online through a radial basis function neural network. The data for the nominal starting weights for the RBFNN have been generated through a modified particle swarm evolutionary procedure. The trained weights are adapted for variations of the plant output from the desired values. Tests carried out show that the proposed adaptive SMES controller maintains the DC capacitor voltage constant thus improving the efficiency of wind energy transfer. The reactive and real power outputs of the SMES improve the voltage profile and the system damping, respectively, following large voltage dips at the grid.

The RBFNN used is simple, easy to generalize, and also provides better approximation of the system nonlinearities in determining the control structure. Training is fast because only a few hidden units need to be updated for a given input. The adaptation process is carried out in time domain, contrary to classical neural network controls. The improvement in the inertia weight swarm optimization technique helps to improve the global exploration and local exploitation abilities. This reduces the effort in creating training data for the neural network significantly.

Acknowledgments This research was sponsored under King Abdel-Aziz City for Science and Technology (KACST) NSTIP Project 11-ENE1632-04 administered through King Fahd University of Petroleum and Minerals (KFUPM). Supports of KACST and KFUPM are acknowledged.

Appendix

PMSG parameters: 1.5 MVA, 690 V, 40-pole, $f_b = 11.5$ Hz, Ra $= 0.01$, $X_d = 1$, $X_q = 0.7$, $H_g = 0.5$ s, $H_t = 3$ s, $K_s = 0.3$, Residual flux $= 0.9$.

Converter circuit parameters: $Ri = 0.05$, $Xi = 0.1$, $C = 1$; Energy storage VSC: Rst $= 0.01$, Lst $= 0.15$, Cdc $= 1$.

Load and line data: $g_L = 0.2$, $b_L = -0.4$, $R_{line} = 0.1$, $X_{line} = 0.2$.

References

1. Uehara, A.; Pratap, A.; Goya, T.; Senjyu, T.; Yona, A.; Urasaki, N.; Funabashi, T: A coordinated control method to smooth wind power fluctuations of a PMSG-based WECS. IEEE Trans. Energy Convers. **26**(2), 550–558 (2011)
2. Sharma, S.; Singh, B.: Control of permanent magnet synchronous generator-based stand-alone wind energy conversion system. IET Power Electron. **5**(8), 1519–1526 (2012)
3. Chinchilla, M.; Arnaltes, S.; Burgos, J.C.: Control of permanent-magnet generators applied to variable-speed wind-energy systems connected to the grid. IEEE Trans. Energy Convers. **21**, 130–135 (2006)
4. Mohd, A.; Ortjohann, E.; Schmelter, A.; Hamsic, N.; Morton, D.: Challenges in integrating distributed energy storage systems into future smart grid. In: 2008 IEEE International Symposium on Industrial Electronics, IEEE, pp. 1627–1632 (2008)
5. Kim, K.H.; Jeung, Y.C.; Lee, D.C.; Kim, H.G.: LVRT scheme of PMSG wind power systems based on feedback linearization. IEEE Trans. Power Electron. **27**(5), 2376–2384 (2012)
6. Haque, M.E.; Negnevitsky, M.; Muttaqi, K.M.: A novel control strategy for a variable-speed wind turbine with a permanent-magnet synchronous generator. IEEE Trans. Ind. Appl. **46**(1), 331–339 (2010)
7. Singh, M.; Khadkikar, V.; Chandra, A.: Grid synchronisation with harmonics and reactive power compensation capability of a permanent magnet synchronous generator-based variable speed wind energy conversion system. IET Power Electron. **4**(1), 122–130 (2011)

8. Wang, L.; Truong, D.N.: Dynamic stability improvement of four parallel-operated PMSG-based offshore wind turbine generators fed to a power system using a STATCOM. IEEE Trans. Power Deliv. **28**(1), 111–119 (2013)
9. Sharma, S.; Singh, B.: Control of permanent magnet synchronous generator-based stand-alone wind energy conversion system. IET Power Electron. **5**(8), 1519–1526 (2012)
10. Bhende, C.N.; Mishra, S.; Malla, S.G.: Permanent magnet synchronous generator-based standalone wind energy supply system. IEEE Trans. Sustain. Energy **2**(4), 361–373 (2011)
11. Chen, S.-S.; Wang, L.; Lee, W.-J.; Chen, Z.: Power flow control and damping enhancement of a large wind farm using a superconducting magnetic energy storage unit. IET Renew. Power Gener. **3**, 23–38 (2009)
12. Ali, M.H.; Tamura, J.: SMES strategy to minimize frequency fluctuations of wind generator system. In: 2008 34th Annual Conference of IEEE Industrial Electronics. IEEE, pp. 3382–3387 (2008)
13. Lu, M.-S.; Chang, C.-L.; Lee, W.-J.: Impact of Wind Generation on a Transmission System. In: 2007 39th North American Power Symposium. IEEE, pp. 348–352 (2007)
14. Batzel, T.D.; Lee, K.Y.: High resolution rotor angle estimation for permanent magnet synchronous machines with Hall effect position sensors using neural networks. Int. J. Eng. Intell. Syst. Elect. Eng. Commun. **8**, 59–65 (2000)
15. Lin, W.; Hong, C.; Oub, T.; Chiu, T.: Hybrid intelligent control of PMSG wind generation system using pitch angle control with RBFN. Energy Conv. Manag. **52**, 1244–1251 (2011)
16. Lee, C.-Y.; Chen, P.-H.; Shen, Y.-X.: Maximum power point tracking (MPPT) system of small wind power generator using RBFNN approach. Expert Syst. Appl. **38**, 12058–12065 (2011)
17. Haris Khan, M.; Rahim A.H.M.A.: IPSO based SMES controller design for a PMSG wind system. In: Proceedings of 2nd IEEE International Energy Conference and Exhibition—ENERGYCON 2012/Future Energy Grids and Systems Symposium, Florence, Italy, 9–12, pp. 599–604 (2012)
18. Suresh, S.: Adaptive neural flight control system for helicopter. In: 2009 IEEE symposium on computational intelligence for security and defense applications. IEEE, pp. 1–8 (2009)
19. Qiu, W.; Fung, K.S.M.; Chan, F.H.Y.; Lam, F.K.; Poon, P.W.F.; Hamernik, R.P.: Adaptive filtering of evoked potentials with radial-basis-function neural network prefilter. IEEE Trans. Biomed. Eng. **49**(3), 225–232 (2002)
20. Arya, L.D.; Titare, L.S.; Kothari, D.P.: Improved particle swarm optimization applied to reactive power reserve maximization. Int. J. Electr. Power Energy Syst. **32**, 368–374 (2010)